International Journal of GEOMATE, Nov., 2017, Vol.13, Issue 39, pp.95-102
Geotec., Const. Mat. & Env., ISSN:2186-2990, Japan, DOI: https://doi.org/10.21660/2017.39.47674

STABILITY CHARTS FOR UNSUPPORTED CIRCULAR TUNNELS IN COHESIVE SOILS

*Jim Shiau[1], Brian Lamb[1], Mathew Sams[1] and Jay Lobwein[1]

[1]School of Civil Engineering and Surveying, University of Southern Queensland, Australia

*Corresponding Author, Received: 2 July 2017, Revised: 11 July 2017, Accepted: 2 Aug. 2017

ABSTRACT: This paper investigates the stability of a plane strain circular tunnel in cohesive soils. A strength reduction technique and the finite difference program *FLAC*, are used to determine the factor of safety for unsupported circular tunnels. Results from the finite difference approach are presented alongside rigorous upper and lower bound limits computed using *Optum G2*. A thorough comparison between these two methods finds very good agreement. As the model is shown to be accurate, design charts are presented for a wide range of practical scenarios using dimensionless ratios. The potential usefulness of this approach is demonstrated using a number of examples. This is considered a simpler way of analysing the stability of an unsupported tunnel that may be as practical as similar methods used in slope stability analysis, such as the commonly used Taylor's design charts.

Keywords: Circular tunnel, Stability, Factor of safety, Undrained clay, FLAC, Optum G2, Strength reduction method, Design chart

1. INTRODUCTION

Growing demands from increased urbanisation and population are driving changes to the way in which transport infrastructure is managed. With limited scope for changes above ground, an increasingly common solution to this is to move more infrastructure and transport below the surface by using tunnels.

For geotechnical engineers, tunnels present some difficulties. The three primary criteria as discussed by Peck [1] are: stability during construction, long and short term settlement, and determination of lining structural loading. This paper will address the stability problem. Correctly analysing the stability of underground infrastructure such as circular tunnels is crucial to prevent the collapse of the structure.

Tunnels have had to be produced in various and increasingly difficult ground conditions from very soft to stiff clays with varying depths of excavation. During tunnel design and construction it is essential to know the soil stability. This is most often known by using the stability number (N) proposed by Broms and Bennermark [2] who initiated a pilot study of the plastic flow of clay soil in vertical openings of retaining walls. Their work was then extended to the experimental study of a tunnel face supported by an internal air pressure in Mair [3]. The stability number is defined in equation 1.

$$N = \frac{\sigma_s - \sigma_t + \gamma(C + D/2)}{S_u} \quad (1)$$

where the surface discharge load is given by σ_s and the internal tunnel pressure is given by σ_t. C is the tunnel cover and D is the tunnel diameter. S_u and γ represent the undrained shear strength and the unit weight of the soil respectively.

Circular tunnel stability using equation 1 has been studied since its origin; see work completed by [3-6]. The studies were largely based on experimental and centrifugal research. Davis et al. [7] built upon the earlier definition of stability ratio and approached the upper and lower bound solutions of the problem using a number of dimensionless parameters. The problem was regarded as to find the limiting value of a pressure ratio $(\sigma_s - \sigma_t)/S_u$ that is a function of the independent parameters such as the depth ratio C/D and the strength ratio $S_u/\gamma D$. With recent development of finite element limit analysis techniques [8-11], a large number of research papers have been published following the definition in [7] in the areas of tunnel stability [13-16]. Recently Shiau [17-19] proposed a pressure relaxation technique using finite different method in *FLAC* that can be used to estimate both settlement and stability problems of tunnelling construction.

It is possible to further simplify this stability number by neglecting σ_s and σ_t. This simulates an unsupported excavation in green-field conditions. With the assumption of σ_s and σ_t both equalling zero, the problem can be reduced to a much simpler factor of safety problem that is a function of the depth ratio C/D and the strength ratio $S_u/\gamma C$ or $S_u/\gamma D$, similar to Taylor's design charts for slope stability analysis [20].

This study uses a strength reduction technique to determine the factor of safety of circular tunnels

in cohesive soils over a wide parametric range. It is the aim of this paper to produce stability charts using the *FoS* approach for practical applications.

2. PROBLEM DEFITION

Tunnelling is a complex phenomenon that is three dimensional in nature. However, it can be simplified to 2D plane strain conditions by taking the transverse section and assuming a very long tunnel. The problem is defined as such in Figure 1. The soil body is modelled as a uniform Mohr-Coulomb material which has both an undrained shear strength (S_u) and unit weight (γ). The circular tunnel is at depth *C* and has a diameter *D*.

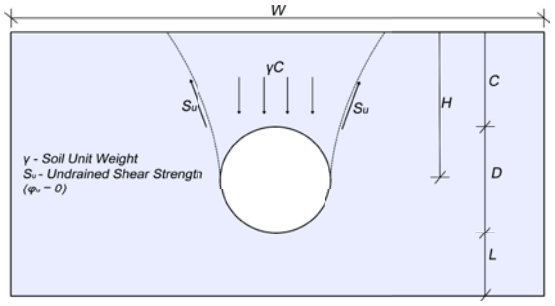

Fig. 1 Problem Definition

The stability of the tunnel is represented using $S_u/\gamma C$ for the first stability design chart produced, and $S_u/\gamma D$ for the second. Factor of safety (*FoS*) in either case, is a function of both stability number and depth ratio, as shown in equations (2) and (3).

$$FoS = f\left(\frac{C}{D}, \frac{S_u}{\gamma C}\right) \quad (2)$$

$$FoS = f\left(\frac{C}{D}, \frac{S_u}{\gamma D}\right) \quad (3)$$

The parameters used in this study are $S_u/\gamma C$ = *0.05 - 1*, $S_u/\gamma D$ = 0.1 - 2 and *C/D = 1 - 6*. This is to cover most of the realistic values to give a comprehensive analysis, and to ensure that the design charts produced can be applicable to many different tunnel design and analysis problems.

By formulating the equation to the problem in this way it allows for the creation of practical stability charts, which are useful for design. These dimensionless ratios allow the results of this study to be used in scenarios that are physically different, but where the soil strength ratio and the depth ratio still fall in the parametric domain.

3. MODELLING TECHNIQUE

Soil mechanics has always been a complex and uncertain discipline. With the development of computers over the last two decades, numerical modelling has proceeded to become a dominant technique for problem resolution. The finite difference method is one such technique that has been successfully used in the past for modelling tunnels, and it has again been used in this study.

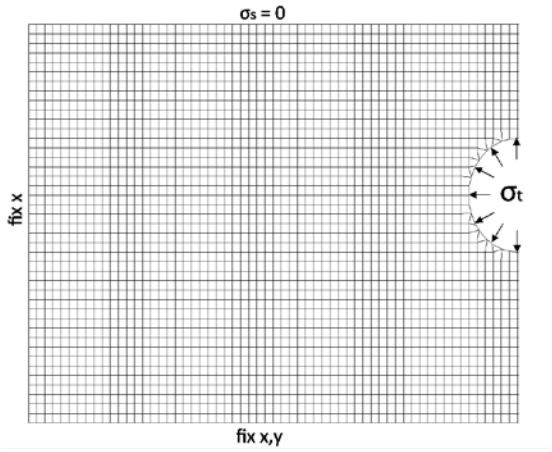

Fig. 2 Typical Mesh

A typical finite difference mesh of the problem in this study is shown in Figure 2. The boundary conditions shown in the figure are important as they ensure that the entire soil mass is modelled accurately despite using a finite mesh. It should be noted that the soil domain size for each of the cases was chosen so that the failure zone of the soil body is placed well within the domain. Using Figure 1, *L = 1.5D* and *W = 6C* are adopted in all analyses of the paper.

With this computer modelling technique, the problem is then solved by using a shear strength reduction methodology. This method is widely known and applied for slope stability analysis, but has rarely been used for tunnel stability analysis. As this method yields a factor of safety (*FoS*), it is believed that this method may provide some practical benefit for designers.

Such a method involving factors of safety has been described by Bishop [21] for slope stability. It is defined as a ratio of the strength necessary to maintain limiting equilibrium with the soil's available strength. The shear strength of the material is reduced until the limiting condition is found. If the material triggers the failure condition initially, then the cohesion and friction angle is increased until the limiting equilibrium or failure state is reached. Therefore the actual and critical strength is known, and the *FoS* can be calculated.

The factor of safety for the many cases being studied are computed by using explicit finite difference code via the software package *FLAC* and the built-in implementation of the strength reduction technique. A dynamic relaxation method

is used explicitly which is integrated step by step with respect to "time". Although the code is based on the explicit finite difference method, it is not very different from a nonlinear finite element program.

An explicit time marching scheme known as dynamic relaxation using the full dynamic equation of motion [22] is adopted to solve the resulting equations which are identical to those in the finite element formulation. To solve a static system using the dynamic equation of motion, an artificial nodal damping is needed so that kinetic energy can be gradually removed. Nodal unbalanced force is one of the many convergence criteria in this explicit method. In order to minimise the initial oscillation of the system, small time stepping is normally adopted [25]. This unavoidably increases the solution time to a certain extent, and requires significant experience and judgement when using this numerical code.

Relying on one single numerical model or any method is normally not convincing, result verification is required. For this purpose, rigorous upper bound and lower bound factors of safety have been calculated using *Optum G2* [26] over the same parametric range. The numerical procedures used in *Optum G2* are based on the limit theorems of classical plasticity; though it uses a similar approach to that in the displacement finite element method to discretise the domain. Finite element implementations of the bound theorems were first proposed by [23] for the lower bound case, and by [24] for the upper bound case. These techniques have continued to be developed in recent times, notably by Sloan [8 & 9] and the many subsequent papers from this method.

4. RESULTS AND DISCUSSION

Using the strength reduction method and the *FLAC* finite difference method as described, results of Factor of Safety (*FoS*) are obtained for unsupported circular tunnels in purely cohesive soil. This study assumes that the soil obeys an associated flow rule and covers two dimensionless parameters, including the depth ratio (*C/D*) and the strength ratio ($S_u/\gamma C$ and $S_u/\gamma D$). The finite difference estimates of the factors of safety are compared with the finite element lower and upper bound estimates computed using *Optum G2*.

4.1 Comparison with rigorous upper and lower bounds

Graphical comparisons are shown in Figures 3 and 4. In general, the finite difference results (shown in dots) are in good agreement with the upper bound solutions (dashed lines), and are consistently 3-5% larger than the lower bound solutions (solid lines). In Figure 3, *FoS* increases linearly as the strength ratio $S_u/\gamma C$ increases, indicating that there exists a stability number where the effective *FoS* is equal to one, a critical stability number (N_c). This could be achieved by dividing the stability ratio ($S_u/\gamma D$ or $S_u/\gamma C$) by the *FoS* result for each case. Also note that the rate of *FoS* increase is different for each *C/D* value. The gradient of the line is greater for higher C/D values.

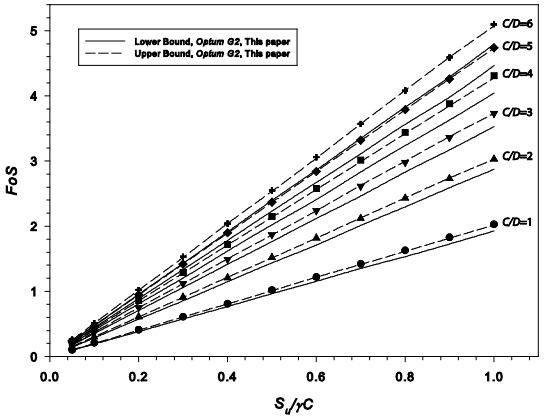

Fig. 3 Comparison of *FoS* results with respect to $S_u/\gamma C$ for various values of *C/D*

Figure 4 shows that *FoS* increases nonlinearly with increasing *C/D* for all strength ratios defined as $S_u/\gamma C$. It should be noted that the strength ratio is normalised with respect to γC, any increase of *C/D* would result in an increase of *C* (*D* is always held constant) and therefore an increase in undrained shear strength.

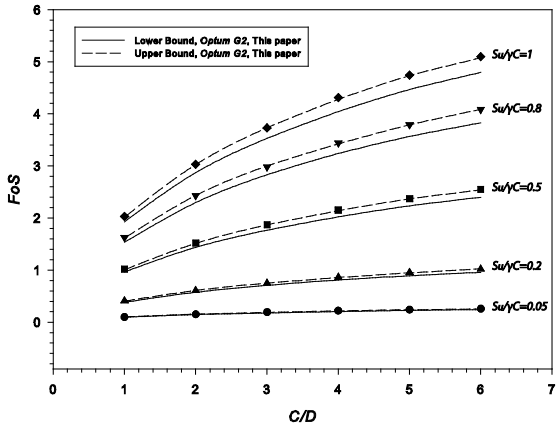

Fig. 4 Comparison of *FoS* results with respect to *C/D* for various values of $S_u/\gamma C$

Figures 5 and 6 are the same charts for the cases defined using the strength ratio $S_u/\gamma D$. In Figure 5, *FoS* decreases nonlinearly with increasing *C/D* for all strength ratios. Figure 6 appears similar to Figure 3. However, the trend with *C/D* is reversed, *FoS*

decreases with *C/D*. The *FoS* also increases as the strength ratio $S_u/\gamma D$ increases. The finite difference results are in good agreement with the upper bound solutions, but again consistently produce results that are 3-5% larger than the lower bound solutions. Note that the strength ratio is normalised with respect to γD. In this way, the undrained shear strength S_u remains constant for all *C/D* values. Owing to the increasing overburden pressure (*C/D* increase), resulting in *FoS* values decreasing. This is in contrast to the widespread belief that an increase to *C/D* sresults in an increase to *FoS*.

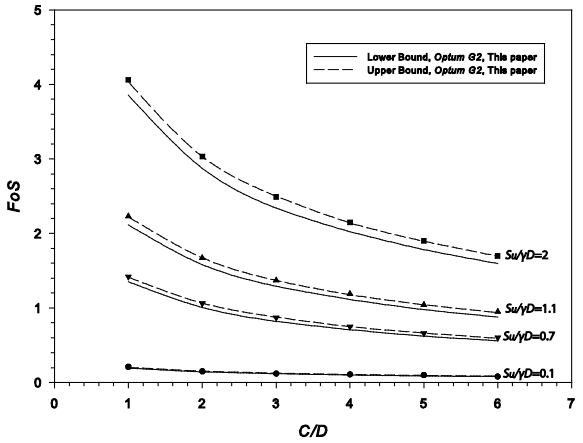

Fig. 5 Comparison of *FoS* results with respect to *C/D* for various values of $S_u/\gamma D$

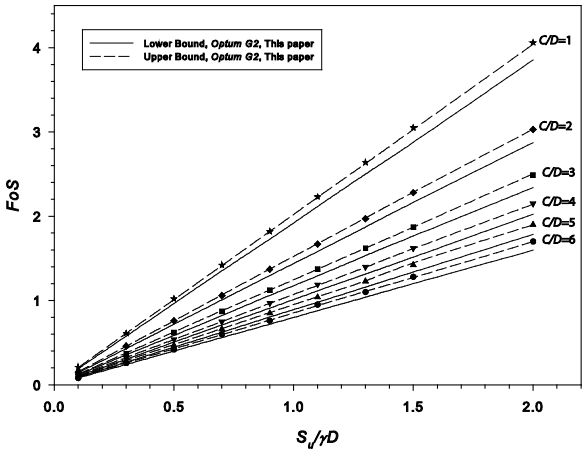

Fig. 6 Comparison of *FoS* results with respect to $S_u/\gamma D$ for various values of *C/D*

4.2 Extent of failure surface

This area of investigation would be related to the type of failure mechanism the circular tunnel will endure at certain depths. Wilson et al. (2011) shows that for shallow tunnels (meaning $C/D \leq 2$) in a homogeneous soil, the failure mode is through the roof and upper sides of the tunnel, whilst for deeper tunnels the failure zone can extend to the base of the tunnel. The weight of the soil constitutes the main load on the circular tunnel, and this is clearly evident with roof top and upper side failures for shallow tunnels.

As the depth ratio (*C/D*) increases, the extents of the failure mechanism increases accordingly. This mechanism is shown in Figure 7. As (*C/D*) increases so does (*E/D*), where *E* is measured from the plots of plastic shear strain rates. It is understood that deeper tunnel instability will result in a wider extent of surface settlement.

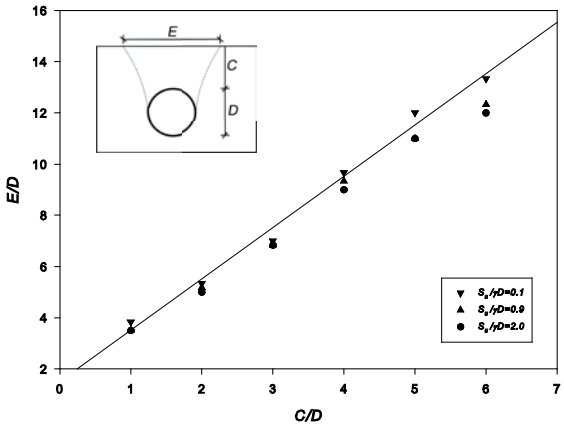

Fig. 7 Effect of *C/D* on the surface extent ratio (*E/D*)

Both soft and stiff undrained clays appear to have the same extent of shear strain rates at failure. Stiffer soils have a smaller magnitude in shear strain rate, simply due to the increased undrained shear strength, while softer soil material having a greater magnitude of shear strain rate at failure. Plots of shear strain rate and velocity field are presented in Figures 8 and 9 for $C/D = 5$ with both $S_u/\gamma C = 0.3$ and $S_u/\gamma C = 0.8$.

5. STABILITY CHART AND PRATICAL USES

The usefulness of the design charts are best demonstrated through a number of examples. Two design contour charts for Factor of Safety (*FoS*) have been constructed in Figures 10 and 11. Selected sample data is also presented in Table 1. For practical design purposes, stability charts can be used by the engineer to relate the depth ratio (*C/D*), soil strength ratio ($Su/\gamma C$ or $Su/\gamma D$), and factor of safety (*FoS*). This is a convenient approach, as all relevant parameters can be observed clearly in one plot. Figure 10 presents the first design chart that is produced for the dimensionless parameters *C/D* and $Su/\gamma C$. Regression of the design chart gives the following relationship with $r^2 = 0.98$,

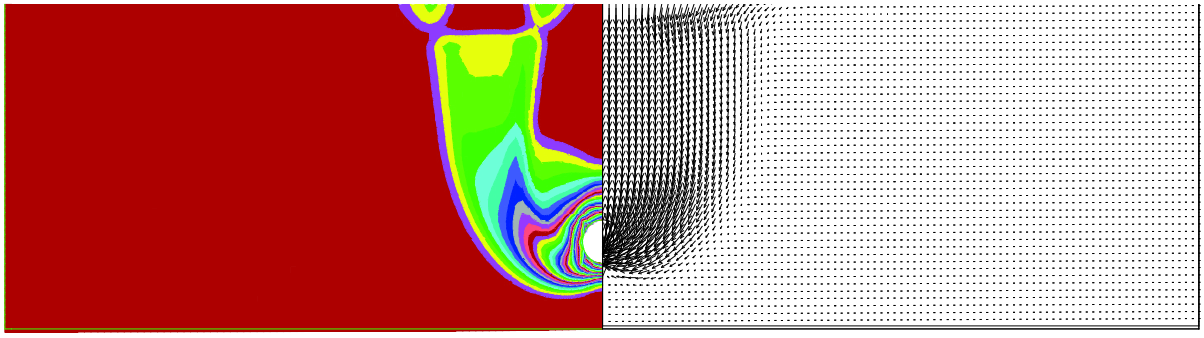

Fig. 8 Plots of shear strain rate and velocity field for C/D=5 and $S_u/\gamma C$ =0.3

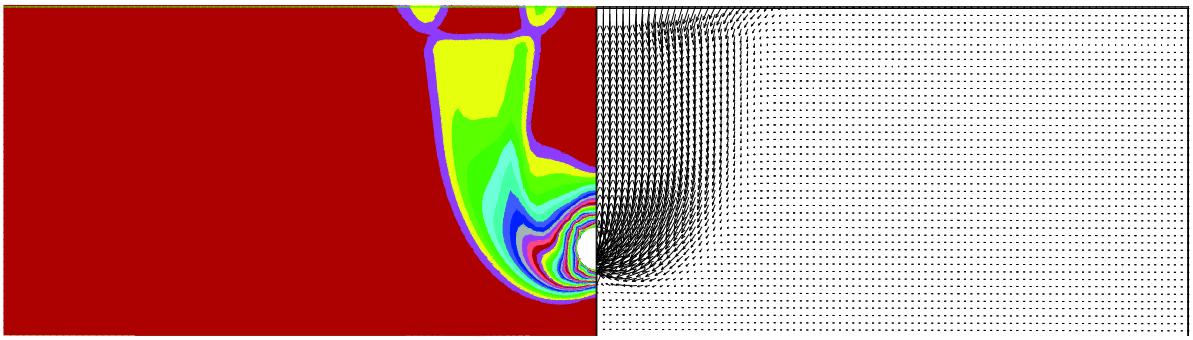

Fig. 9 Plots of shear strain rate and velocity field for C/D=5 and $S_u/\gamma C$ =0.8

$$FoS = 2\left(\frac{S_u}{\gamma C}\right)\sqrt{\left(\frac{C}{D}\right)} \quad (4)$$

Figure 11 presents the second design chart that is produced for the dimensionless parameters C/D and $S_u/\gamma D$. Regression of the design chart gives the following relationship with $r^2 = 0.96$,

$$\boldsymbol{FoS = \frac{S_u}{\gamma D}\left(\frac{1}{0.133\left(\frac{C}{D}\right)+0.4}\right)} \quad (5)$$

5.1 The Stability Charts

The chart in Figure 10 conforms to the widely accepted truth that FoS increases with C/D. However, it can be seen that this trend isn't followed in Figure 11, where it appears that the FoS decreases with C/D. This is in fact due to the definition of the soil strength ratio ($S_u/\gamma C$ and $S_u/\gamma D$) and the modelling methodology that has been used. The diameter is held constant through all cases and the overburden (C) is changed. In Figure 10, the actual shear strength of the soil increases with C/D. As the tunnel diameter is held constant in all cases, the actual soil strengths in Figure 11 remain constant regardless of C/D.

Should the solution procedure be such that the tunnel cover (C) remained constant and the diameter was the changing parameter, the trends of the two design charts would be vice-versa. Another consequence of defining the soil strength ratio as in Figure 10, is that the actual shear strengths used become increasingly divergent with higher C/D ratios. This results in diminishing accuracy at greater depth ratios. Despite this, it may still be reasonably expected that both charts conform to the expected trend.

The problem can be better understood if it is considered in terms of active and resisting forces. This is shown in Figure 1, where the active force is the weight of soil and the resisting force is given by the shear strength of the soil. A simple observation can be made from this; of two hypothetical tunnels in the same cohesive soil but at different depths, the tunnel with the smaller active force (γC) will be more stable.

This observation may not be true in a soil with internal friction due to material stress redistribution and geometrical arching effects. In purely cohesive soils, the latter still occurs, but its effect is not enough to overcome that subsequent increase in active force.

5.2 Examples

Using the two design charts and the two regressed equations, some practical uses become apparent. These can be broadly categorized either analysis or design.

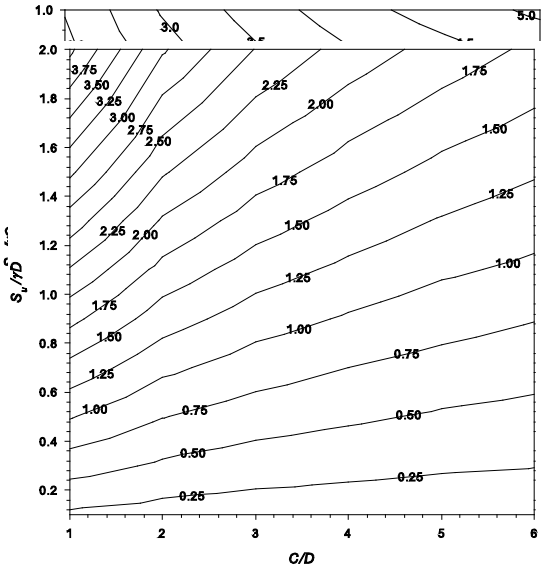

Fig. 10 *FoS* stability chart for *C/D* and $S_u/\gamma C$
Fig. 11 *FoS* stability chart for *C/D* and $S_u/\gamma D$

5.2.1 Analysis of an existing unsupported tunnel

For an existing unsupported tunnel with no surcharge load ($\boldsymbol{\sigma_s}$) and no capacity to provide internal supporting pressure ($\boldsymbol{\sigma_t}$), determine the factor of safety of the tunnel given the parameters S_u = 50 kPa, γ = 18 kN/m^3, C = 5 m, and D = 2 m.

1. Using C/D = 2.5, $S_u/\gamma C$ = 0.56, equation 4 gives a *FoS* of 1.77.
2. Using C/D = 2.5, $S_u/\gamma C$ = 0.56, figure 10 gives an approximate *FoS* of 1.81.

Alternatively,

1. Using C/D = 2.5, $S_u/\gamma D$ = 1.39, equation 5 gives a *FoS* of 1.90.
2. Using C/D = 2.5, $S_u/\gamma D$ = 1.39, figure 11 gives an approximate *FoS* of 1.88.

An actual computer analysis of this particular case gives a *FoS* of 1.93.

5.2.2 Design of an unsupported tunnel

In the case of designing an unsupported tunnel, which is likely to be only temporary in most cases, a target *FoS* needs to be achieved. For this scenario, the soil properties are normally known and the required diameter is specified.

Table 1 – Comparison of *FLAC* with *Optum G2* *FoS* results

C/D	$S_u/\gamma D$	*FLAC* (Finite Difference) *SSRM**	*Optum G2* (Limit Analysis) Upper Bound, *SSRM**	*Optum G2* (Limit Analysis) Lower Bound, *SSRM**
4	0.1	0.11	0.107	0.101
	0.3	0.32	0.321	0.301
	0.5	0.54	0.535	0.505
	0.7	0.75	0.748	0.708
	0.9	0.97	0.962	0.907
	1.1	1.19	1.176	1.113
	1.3	1.40	1.391	1.312
	1.5	1.62	1.612	1.513
	2	2.15	2.139	2.022
5	0.1	0.10	0.095	0.089
	0.3	0.28	0.284	0.266
	0.5	0.47	0.474	0.446
	0.7	0.66	0.663	0.622
	0.9	0.85	0.853	0.803
	1.1	1.04	1.042	0.978
	1.3	1.23	1.229	1.158
	1.5	1.42	1.442	1.337
	2	1.90	1.894	1.783
6	0.1	0.08	0.085	0.080
	0.3	0.26	0.255	0.239
	0.5	0.42	0.423	0.399
	0.7	0.60	0.592	0.559
	0.9	0.76	0.762	0.717
	1.1	0.95	0.936	0.878
	1.3	1.10	1.105	1.038
	1.5	1.28	1.269	1.199
	2	1.70	1.693	1.595

** Shear Strength Reduction Method (SSRM)*

The designer needs to determine the overburden (C) required for to meet the desired factor of safety. If the following is known: S_u = 50 kPa, γ = 18 kN/m^3, D = 2 m, and *FoS* = 1.50, determine the required tunnel cover C.

1. Using *FoS* = 1.50 and $S_u/\gamma D$ = 1.39, equation 5 gives a C value of 7.92 m.
2. Using *FoS* = 1.50 and $S_u/\gamma D$ = 1.39, Figure 11 gives an approximate C/D value of 4.0 and therefore C value of 8.0 m.

An actual computer analysis for this particular case (C value of 8.0m) gives a *FoS* of 1.51.

Alternatively,

1. Using FoS = 1.50, S_u = 50 kPa, γ = 18 kN/m^3, D = 2 m, equation 4 gives C = 6.9 m.
2. Using the chart in Figure 10 will require an iterative solution by 'trial and error'. The use of equation is recommended for this situation.

An actual computer analysis of this particular case (C value of 6.9m) gives a FoS of 1.64.

6. CONCLUSION

Stability of plane strain circular tunnels was investigated in this paper using a factor of safety approach. Numerical results of FoS were obtained by using a shear strength reduction method in both a finite difference method *(FLAC)* and a rigorous upper and lower bound limit analysis (*OptumG2*). The comparison of the results from both of these numerical approaches were very promising. Design charts were then produced using dimensionless ratios. Some examples to illustrate the usefulness have been given; they can be used in both the design and analysis of unsupported tunnels.

The FoS approach to tunnel stability provides an alternative option for the designer and is a useful approach in that the factors of safety always provide direct information and understanding of tunnel stability. Further research is required on how this method can be applied to tunnels with a non-zero surcharge (σ_s) and internal pressure (σ_t).

7. AUTHOR'S CONTRIBUTIONS

This project was conducted by USQ Tunnel Modeling Group in Australia since 2010 under the leadership of Dr. Jim Shiau who has developed the process and scripts to simulate underground tunnel construction and design for stability and settlement problems. The co-authors Brian Lamb, Mathew Sams and Jay Lobwein were involved in this research during their study period in Bachelor's and Master's degree at USQ.

8. ETHICS

This article is original and contains unpublished material. The corresponding author confirms that all of the other authors have read and approved the manuscript and no ethical issues or conflict of interests involved.

9. REFERENCES

[1] Peck, RB 1969, 'Deep excavations and tunneling in soft ground', Proceedings of 7th International Conference on Soil Mechanics and Foundation Engineering, Mexico City. Mexico, pp. 225-298.

[2] Broms, BB & Bennermark, H 1967, 'Stability of clay at vertical openings', Journal of the Soil Mechanic and Foundations Division, Proceedings of the American Society of Civil Engineers, vol. 93, pp. 71- 93.

[3] Mair RJ 1979, 'Centrifugal modelling of tunnel construction in soft clay', PhD thesis, University of Cambridge.

[4] Cairncross AM 1973, 'Deformation around model tunnels in stiff clay', PhD thesis, University of Cambridge.

[5] Atkinson JH & Cairncross AM 1973. 'Collapse of a shallow tunnel in a Mohr-Coulomb material. In: Role of plasticity in soil mechanics', Cambridge, p. 202–06.

[6] Seneviratne HN 1979. 'Deformations and pore-pressures around model tunnels in soft clay', PhD thesis, University of Cambridge.

[7] Davis, EH, Gunn, MJ, Mair, RJ & Seneviratne, HN 1980, 'The stability of shallow tunnels and underground openings in cohesive material', Geotechnique, vol. 30, pp. 397-416.

[8] Sloan, SW 1988, 'Lower bound limit analysis using finite elements and linear programming', International Journal for Numerical and Analytical Methods in Geomechanics, vol. 12, pp. 61-67.

[9] Sloan, SW 1989, 'Upper bound limit analysis using finite elements and linear programming', International Journal for Numerical and Analytical Methods in Geomechanics, vol. 13, pp. 263-282.

[10] Lyamin, AV, & Sloan, SW 2002a, 'Lower bound limit analysis using non-linear programming', International Journal for Numerical Methods in Engineering, vol. 55, no. 5, pp. 573-611.

[11] Lyamin, AV & Sloan, SW 2002b, 'Upper bound limit analysis using linear finite elements and non-linear programming', International Journal for Numerical and Analytical Methods in Geomechanics, vol. 26, no. 2, pp. 181-216.

[12] Wilson, DW, Abbo, AJ, Sloan, SW, Lyamin & AV 2011, 'Undrained stability of a circular tunnel where the shear strength increase linearly with depth', Canadian Geotechnical Journal, NRC Research Press, vol. 48, pp. 1328-1342.

[13] Wilson, DW, Abbo, AJ, Sloan, SW, & Lyamin,

AV 2013, 'Undrained stability of a square tunnel where the shear strength increases linearly with depth', Computers and Geotechnics, vol.49, pp.314-325.

[14] Wilson, DW, Abbo, AJ, Sloan, SW, & Lyamin, AV 2014, 'Undrained Stability of Dual Circular Tunnels', International Journal of Geomechanics, vol. 14(1), pp. 69-79.

[15] Yamamoto, K, Lyamin, AV, Wilson, DW, Sloan, SW & Abbo, AJ 2011b, 'Stability of a single tunnel in cohesive–frictional soil subjected to surcharge loading', Canadian Geotechnical Journal, NRC Research Press, vol. 48, no. 12, pp. 1841-1854.

[16] Yamamoto, K, Lyamin, AV, Wilson, DW, Sloan, SW & Abbo, AJ 2011a, 'Stability of a circular tunnel in cohesive-frictional soil subjected to surcharge loading', Computers and Geotechnics, vol. 38, pp. 504-514.

[17] Shiau, J. S., Sams, M. S., & Lamb B. (2016). Introducing Advanced Topics in Postgraduate Geotechnical Engineering Education – Tunnel Modelling. International Journal of Geomate, 10(1): 1698-1705.

[18] Shiau, J. S., Lamb B., & Sams, M. S. (2016). The use of sinkhole models in advanced geotechnical engineering teaching. International Journal of Geomate, 10(2): 1718-1724.

[19] Shiau, J. S., Sams, M. S., & Chen J. (2016). Stability Charts for a Tall Tunnel in Undrained Clay. International Journal of Geomate, 10(2): 1764-1769.

[20] Taylor, DW 1937, 'Stability of earth slopes.' Journal of the Boston Society of Civil Engineers, vol. 24, no. 3, pp. 197-246.

[21] Bishop, AW 1955, 'The use of slip circle in the stability analysis of slopes', Geotechnique, vol. 5(1), pp. 7-17.

[22] Otter, JRH, Cassell, AC & Hobbs, R E 1966, 'Dynamic relaxation', Proceedings of the Institution of Civil Engineers, Vol: 35, pp. 633-656.

[23] Lysmer J 1970, 'Limit analysis of plane problems in soil mechanics', ASCE Journal of the Soil Mechanics and Foundations Division, vol. 96, pp. 1311–34.

[24] Anderheggen E & Knopfel H 1972, 'Finite element limit analysis using linear programming', International Journal of Solids and Structures, vol. 8, pp. 1413–31.

[25] FLAC 2003, Fast Lagrangian Analysis of Continua, Version 4.0, Itasca Consulting Group, Minneapolis, Minnesota, USA.

[26] Optum G2 2013, Optum Computational Engineering, Version 1.2014.10.1, Newcastle, Australia.